

Article

Effect of Novel Micro-Arc Oxidation Implant Material on Preventing Peri-Implantitis

Xiaoyu Huang^{1,2,3}, Wen Zhou^{1,2,3}, Xuedong Zhou^{1,2,3}, Yao Hu^{1,2,3}, Pengfei Xiang^{1,2,3}, Bolei Li^{1,2,3}, Bangcheng Yang⁴, Xian Peng^{1,3}, Biao Ren^{1,3}, Mingyun Li^{1,3,*} and Lei Cheng^{1,2,3,*} 

¹ State Key Laboratory of Oral Diseases, Sichuan University, Chengdu 610064, China; 2013181641007@stu.scu.edu.cn (X.H.); wzhou1@umaryland.edu (W.Z.); zhouxid@scu.edu.cn (X.Z.); 2018324035065@stu.scu.edu.cn (Y.H.); 2017224035068@stu.scu.edu.cn (P.X.); 2018324035063@stu.scu.edu.cn (B.L.); pengx@scu.edu.cn (X.P.); renbiao@scu.edu.cn (B.R.)

² Department of Operative Dentistry and Endodontics, West China School of Stomatology, Sichuan University, Chengdu 610064, China

³ National Clinical Research Centre for Oral Diseases, Sichuan University, Chengdu 610064, China

⁴ National Engineering Research Center for Biomaterials, Sichuan University, Chengdu 610065, China; yangbcheng@126.com

* Correspondence: limingyun@scu.edu.cn (M.L.); chenglei@scu.edu.cn (L.C.)

Received: 3 September 2019; Accepted: 21 October 2019; Published: 23 October 2019



Abstract: Dental implants occasionally fail for many reasons, especially peri-implantitis. The adhesion of bacteria to the surface of titanium is the initial factor in peri-implantitis. Therefore, the aim of this study was to assess the effect of a novel micro-arc oxidation (MAO) titanium on bacteria inhibition and regulation through periodontitis, and on a healthy saliva-derived biofilm, in vitro. MAO, sandblasting and acid etching (SLA), machined titanium and plasma-sprayed hydroxyapatite (HA) were selected for further study. The metabolic activity and biomass accumulation were tested using MTT (3-(4,5-Dimethyl-thiazol-2-yl)-2,5-diphenyltetrazolium bromide) and crystal violet assay after 24 h of anaerobic incubation. The structure was determined by scanning electron microscopy (SEM) and live/dead staining. Moreover, 16S rDNA sequencing was used to assess the microbial community. The results showed that biofilms on MAO were thinner compared to HA and SLA. In the periodontitis group, the biofilm accumulation and metabolic activity reached the highest levels in the HA group ($p < 0.05$); MAO titanium had the smallest biofilm accumulation and higher live/dead ratio; and the relative abundance of *Lactobacillus* in the SLA, HA and MAO groups increased significantly compared to the machined group ($p < 0.05$). In the healthy group, the relative abundance of *Lactobacillus* in the MAO group increased significantly compared to the other three groups ($p < 0.05$); the amount and metabolism activity of bacteria in the MAO group was lower ($p < 0.05$); MAO titanium had the least biofilm accumulation and a higher live/dead ratio. In conclusion, the novel MAO titanium had the ability to combat peri-implantitis by inhibiting the biofilm and regulating the microbial ecosystem to healthier conditions.

Keywords: biofilms; dental implant; micro-arc oxidation; peri-implantitis; titanium

1. Introduction

Dental implants are widely used for reconstruction, for functional and aesthetic problems, in partially and fully edentulous patients. Although dental implants are a predictable treatment option, they occasionally fail for a variety of reasons [1]. One reason is peri-implantitis, which is a late complication of dental implants and the primary process that leads to late failure [2]. Peri-implantitis has been reported to occur in 15.3% of patients and 9.2% of implants [3]. Moreover, to treat peri-implantitis,

patients need to pay around 332.87 euros more for each implant than healthy individuals [4]. Therefore, peri-implantitis is a worldwide health problem, due to the prevalence of dental implants.

In the current study, we confirmed that peri-implantitis was caused by polymicrobial synergy and dysbiosis, and the adhesion of oral microorganisms to the titanium surface was the initial factor of peri-implantitis [5]. Many risk indicators influenced the equilibrium between the host and its commensal microbiota, sometimes leading to dysbiosis, which gave rise to oral microbial-shift diseases such as peri-implantitis [5]. Periodontitis was one of the most important risk factors for peri-implantitis. It has been reported that the failure rate of implantation with periodontitis was as high as 25.0% and the incidence of peri-implantitis as high as 66.7% [6]. Periodontitis led to an increased incidence of peri-implantitis, mainly because periodontitis brought about a change in the microflora around the implant, and the microflora of periodontitis was beneficial to the occurrence of peri-implantitis [7–10]. However, some bacterial strains, such as *Lactobacillus*, a probiotic for peri-implant diseases, could help regulate the micro ecosystem and lead to a healthier biofilm [11–13].

Dental implants are ideal for bacterial colonization and biofilm formation [14,15]. The microorganisms expressed different genes, to adapt to environments, when they grew on different materials, which eventually led to differences in their micro ecology [16]. It has been shown that the surface roughness of the implant could affect the adhesion of oral bacteria [17]. Different implant materials, such as titanium, titanium alloys, and zirconia could also influence the adhesion and metabolism of bacteria, and even the components of the biofilm [15,18,19]. Plasma-sprayed hydroxyapatite (HA), and sandblasting and acid etching (SLA) are two common surface treatments for clinical commercial titanium implants. Although they had acceptable osseointegration ability [20,21], they all showed increased adhesion of bacteria [22]. Micro-arc oxidation treatment is a method to establish the oxide film on a metal surface through discharge oxidation, which showed better osteogenic characteristics and had potential antibacterial abilities because of its uniform surface.

Therefore, to prevent peri-implantitis, our ideal material would reduce the adhesion of bacteria, especially several pathogenic bacteria. Therefore, we developed a novel micro-arc oxidation (MAO) implant material, which is expected to reduce the adhesion of bacteria and the risk of peri-implantitis, especially the risk of peri-implantitis in high-risk groups such as periodontitis patients.

2. Materials and Methods

2.1. Preparation of Titanium Discs

Titanium discs 6 mm in diameter and 1 mm in thickness were prepared. Four types of treatment, SLA, HA, MAO, and a machined technique, were applied to the surface of the titanium discs. SLA was first processed by sandblasting treatment by Al_2O_3 particles, and then etched in an acid solution (sulfuric acid: hydrochloric acid: H_2O = 1:1:2). HA was first sandblasted and then plasma-sprayed with 30 μm of hydroxyapatite. The machined technique was mechanically polished in sequence with grit SiC paper (#180, #400, #800, #1200) [23]. The novel MAO was connected to the anode of an anodizing device and immersed into a $1 \text{ mol}\cdot\text{L}^{-1}$ H_2SO_4 solution for anodic oxidation treatment by applying a DC voltage of 70 V for 1 min [24]. Finally, the titanium discs were sterilized in an ethylene oxide sterilizer (Anprolene AN 74i, Andersen, Haw River, NC, USA).

2.2. Saliva Collection

This study was authorized by the Ethical Committee of West China School of Stomatology, Sichuan University (Chengdu, China, WCHSIRB-D-2018-020). Ten healthy individuals without active caries or periodontal disease and with natural dentition served as donors for healthy saliva. Ten periodontitis patients diagnosed with chronic periodontitis, according to the American Periodontal Association standard for classification and diagnosis of periodontal disease, were selected as donors for periodontitis saliva. Donors did not take any antibiotics in the three months previous to the study and were starved 2

h before sample collection. Moreover, when saliva was collected, donors gargled with water. The saliva was pooled and diluted two-fold with sterile 50% glycerol. Then the saliva was stored at $-80\text{ }^{\circ}\text{C}$ [25,26].

2.3. Biofilm Development

Every sterile disc was placed into a well of the polystyrene 24-well flat-bottomed microtiter plate, after which 1.5 mL SHI medium was added, as previously described by [27]. The saliva-glycerol stock was seeded (1:50 final dilution) into plates and incubated at $37\text{ }^{\circ}\text{C}$ for 24 h under anaerobic conditions (90% N_2 , 5% CO_2 , 5% H_2). The medium was refreshed every 12 h. After 24 h, phosphate-buffered saline (PBS) was used to rinse the biofilms to remove loose bacteria before immersing in a fresh medium [28].

2.4. SEM, AFM and EDX Observation

For the scanning electron microscopy (SEM) examination of the titanium discs surfaces, the titanium discs were sputter-coated with gold, as previously described by [29]. For the biofilms, the PBS-rinsed biofilms on the disks were immersed in 2.5% glutaraldehyde overnight at $4\text{ }^{\circ}\text{C}$. The discs were then washed twice in sterile water, dehydrated using ethanol solutions (50%, 60%, 70%, 80%, 90% and 100%), and sputter-coated with gold. Finally, SEM (SEM, Quanta 200, FEI, Hillsboro, OR, USA) was used to examine the biofilms. The morphologies of the samples were observed by SEM equipped with energy dispersive spectrometry (EDX, Oxford, UK). The results of the element analysis were obtained with INCA Energy software (INCA PentaFET×3) by Oxford Instruments.

An atomic force microscope (AFM, 5500 SPM, Agilent, Santa Clara, CA, USA) was used at high resolution with a sharp silicon tip in tapping model. Three random fields were selected to obtain surface topography of each specimen and surface average roughness (Ra) values. The 3-dimensional (3D) morphological reconstructions of the specimens were obtained by systemic software (SPIWIN 2.0, Seiko, Tokyo, Japan). Three specimens were tested for each group respectively.

2.5. Crystal Violet Assay

To analyze biomass accumulation, a crystal violet assay was performed according to a previous study with some modifications [25]. Briefly, each group included nine duplicate samples. The PBS-rinsed 24 h biofilms were placed into a 24-well plate. To fix the biofilm, 1 mL 95% methyl alcohol was added to each well and incubated for 15 min. Then, the biofilms were rinsed with PBS, transferred to a new 24-well plate, and submerged in 1 mL 0.1% crystal violet solution for 30 min. To remove the residual dye, the biofilms were washed with PBS. The discs were then transferred to another 24-well plate. A total of 2 mL 95% ethanol solution was added to each well and the plate was shaken at 80 rpm for 45 min at room temperature. Subsequently, 200 μL ethanol of the solution from each well was transferred to a 96-well plate, and a microplate reader was used to measure the absorbance of the solution at a wavelength of 595 nm.

2.6. MTT Assay

To measure the metabolic activity, the MTT (3-(4,5-Dimethyl-thiazol-2-yl)-2,5-diphenyltetrazolium bromide) assay was used [30]. Each group involved nine duplicate samples. After proliferation for 24 h, the biofilms were rinsed with PBS and placed in a 24-well plate with 1 mL MTT dye per well (0.5 mg/mL MTT in PBS). Then, the biofilm plates were anaerobically cultured for 1 h at $37\text{ }^{\circ}\text{C}$. The discs were placed into a new 24-well plate filled with 2 mL dimethyl sulfoxide (DMSO) and shaken at 80 rpm for 20 min in the dark to dissolve the formazan crystals. Finally, 200 μL of DMSO, solution containing the formazan crystals retained by the biofilms was placed into a 96-well plate, and the absorbance was read at a wavelength of 540 nm using a microplate reader.

2.7. Live/Dead Staining

The biofilm was rinsed with PBS before being drained of water and stained using the BacLight live/dead bacterial viability kit (Molecular Probes, Eugene, OR, USA) for 15 min in the dark [31]. Live bacteria cells emitted green fluorescence, while dead cells were stained with propidium iodide and emitted red fluorescence. The biofilms were observed using confocal laser scanning microscopy (Leica, Wetzlar, Germany). Each sample was evaluated randomly at at least 3 sites and experiments were independently performed in triplicate. The ratio between live and dead bacterial cells and biofilm thickness was performed using Image-Pro Plus 6.0 (Media Cybernetics, Bethesda, MD, USA) and Matrix Laboratory (Mathworks, MA, USA) by calculating the relative fluorescence.

2.8. 16S rDNA Sequencing

Biofilms were subjected to Majorbio (Shanghai, China) and total DNA was isolated, amplified, and sequenced according to the standard procedures [27,32]. Briefly, the DNA was first extracted from the saliva-derived biofilms by the E.Z.N.A.[®] Soil DNA Kit (Omega Bio-tek, Norcross, GA, USA). Nanodrop (Thermo Scientific, Wilmington, NC, USA) and agarose gel electrophoresis were used to assess the DNA concentration and quality, respectively. To amplify the variable region 4 and 5 (V4–V5) of bacterial 16S rRNA by PCR, 515F_907R, barcoded primers were used. This procedure was performed in triplicate in a 20 μ L mixture containing 4 μ L of 5 \times FastPfu Buffer, 2 μ L of 2.5 mM dNTPs, 0.8 μ L of each primer (5 μ M), 0.4 μ L of FastPfu Polymerase, and 10 ng of template DNA. Then, the amplicons were extracted from 2% agarose gels, purified by the AxyPrep DNA Gel Extraction Kit (Axygen Biosciences, Union, CA, USA) and quantified by QuantiFluor[™]-ST (Promega, Madison, WI, USA). Using an Illumina MiSeq platform, purified amplicons were paired-end sequenced (2 \times 300) according to the manufacturer's guidelines. Raw data were uploaded to the NCBI Sequence Read Archive (SRA) database.

2.9. Bioinformatics and Statistical Analysis

Raw FASTQ files were demultiplexed and quality-filtered by QIIME (version 1.9.1) [33]. Operational taxonomic units (OTUs) were clustered with a 98.5% similarity cutoff based on UPARSE (version 7.1). The taxonomy of each 16S rRNA gene sequence was analyzed by the Ribosomal Database Project (RDP) Classifier (<http://rdp.cme.msu.edu/>) against the Human Oral Microbiome Database (HOMD) with a confidence threshold of 70% [34,35]. Alpha diversity index (Simpson index) calculations were performed using Mothur v.1.30.2. Phylogenetic beta diversity was determined based on the represented sequences of OTUs. Principal component analysis (PCA) was conducted according to the distance matrices determined by the represented sequences of OTUs for each sample.

Mann–Whitney U tests were performed to detect the significant effects of the variables at a *p*-value of 0.05. For statistical analyses, SPSS version 21.0 (SPSS Inc., Chicago, IL, USA) software was used.

3. Results

3.1. Scanning Electron Microscopy (SEM) Observation of the Surface of Titanium Discs

The surface structures of four types of titanium discs (HA, SLA, MAO, and machined) are presented in Figure 1. The HA discs demonstrated a coarser surface compared to the MAO and machined discs, and crystals were observed in the surface of HA titanium discs. Of these four types of titanium discs, the MAO titanium discs showed a homogeneous microstructure. The surface element composition of the HA discs was C, O, P and Ca. The surface of MAO discs consisted of O and Ti. The SLA and machined discs contained only Ti.

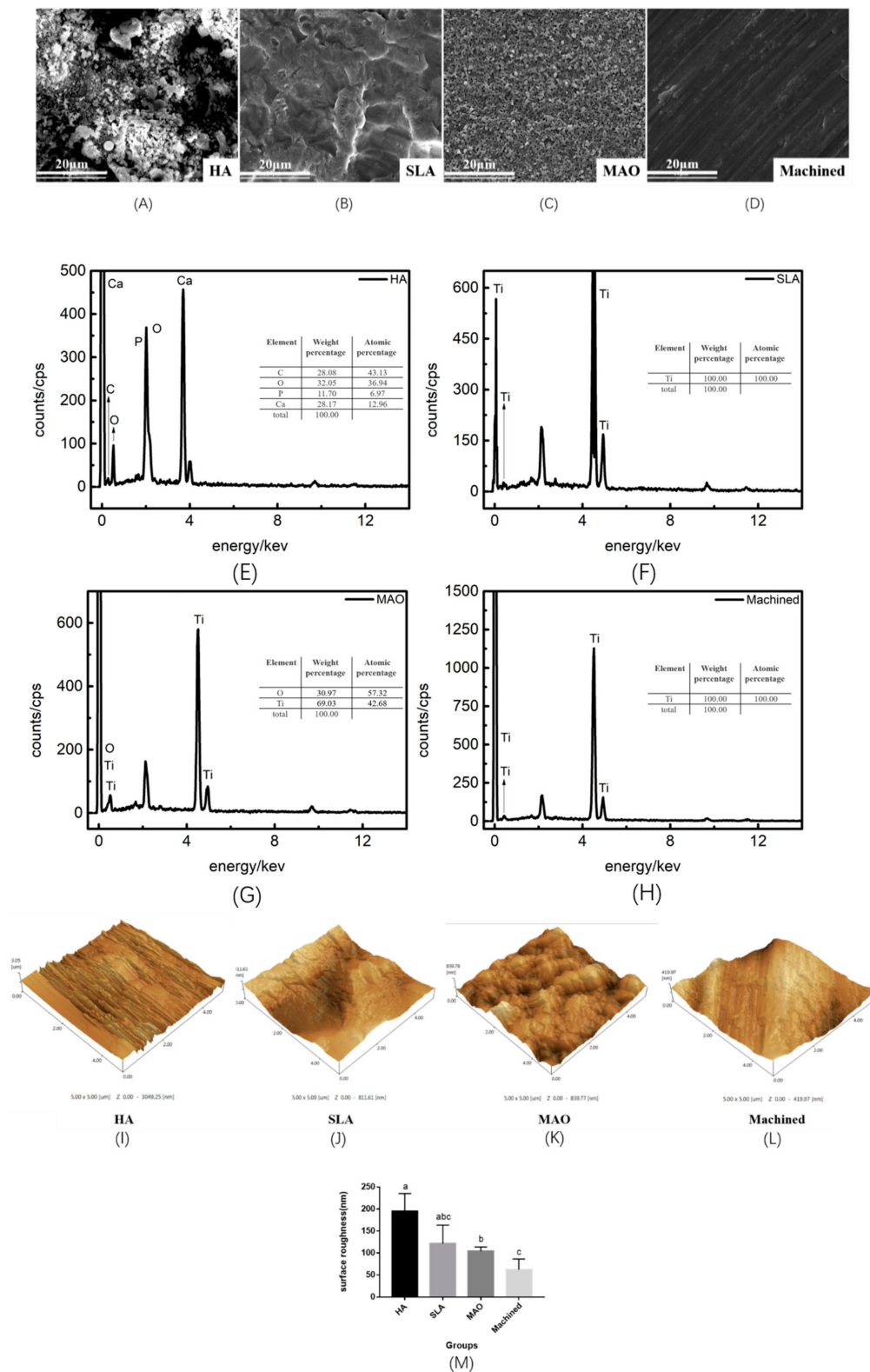


Figure 1. The surface structures of four types of titanium discs (plasma hydroxyapatite spraying (HA), sandblasting and acid etching (SLA), micro-arc oxidation (MAO), and machined) were observed by scanning electron microscopy (SEM), atomic force microscope (AFM) and energy dispersive X-Ray spectroscopy (EDX). (A,E,I) HA: plasma-sprayed hydroxyapatite; (B,F,J) SLA: sandblasting and acid etching; (C,G,K) MAO: micro-arc oxidation; (D,H,L) machined; and (M) the surface roughness of titanium. Significant differences between the bars are marked with different letters (a, b, and c) ($p < 0.05$).

3.2. Scanning Electron Microscopy Observation of Biofilm on Titanium Discs

The structure of biofilms on titanium discs is displayed in Figure 2. The structure of the biofilms was different between each group, as was the morphology of the bacteria. There were many *Coccus* and only a few *Bacillus* present on the titanium.

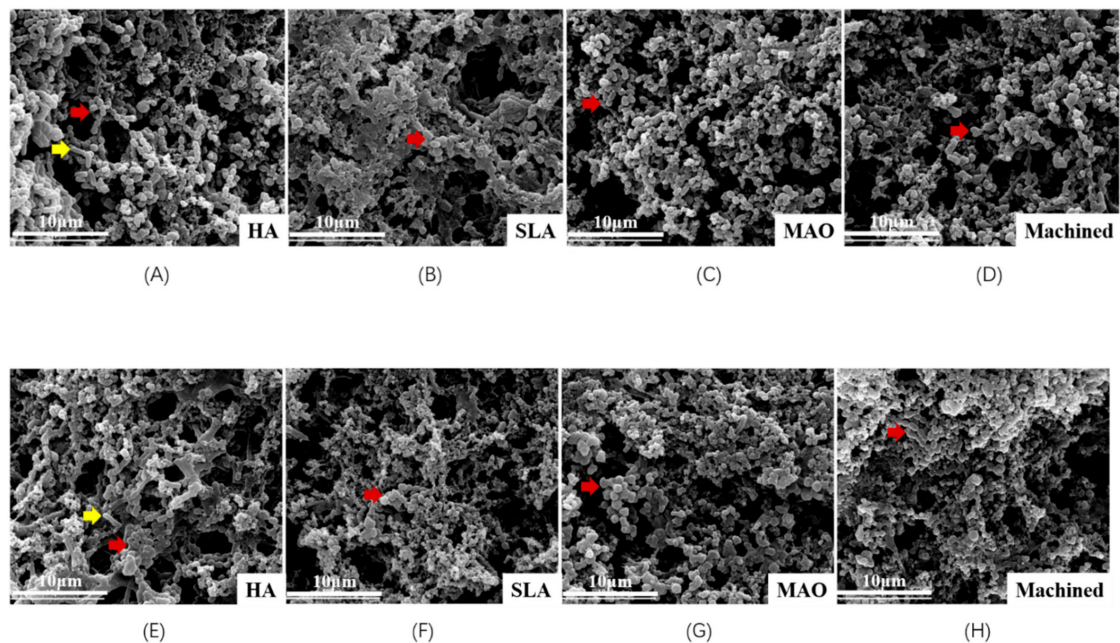


Figure 2. The structure of saliva-derived biofilms (periodontitis and health) on titanium discs was observed by scanning electron microscopy (SEM). (A–D) Periodontitis saliva-derived biofilms on HA, SLA, MAO, and machined titanium; and (E–H) healthy saliva-derived biofilms on HA, SLA, MAO, and machined titanium. The red arrows indicate *Coccus* while the yellow arrows indicate *Bacillus*.

3.3. Metabolic Activity and Biomass Accumulation

The biomass of the metabolic activity of saliva-derived biofilms is presented in Figure 3A,B. In the periodontitis group, compared with the HA group, the metabolic activity of the biofilms on the SLA, MAO, and machined group decreased significantly ($p < 0.05$). No significant differences were observed between the SLA, MAO, and machined group. In the healthy group, the metabolic activity of the biofilms in the MAO group was lower than that of the HA group ($p < 0.05$), and no significant differences were observed between the SLA, MAO, and machined group. Furthermore, between the HA, SLA, and machined group, no significant differences were observed.

The biomass accumulation of saliva-derived biofilms was assessed using crystal violet assay, and is presented in Figure 3C,D. In the group with periodontitis, the HA group showed significantly increased biomass accumulation compared to the other three groups ($p < 0.05$). The results of the healthy group were similar to that of the periodontitis group, although the HA group showed more biofilm accumulation ($p < 0.05$).

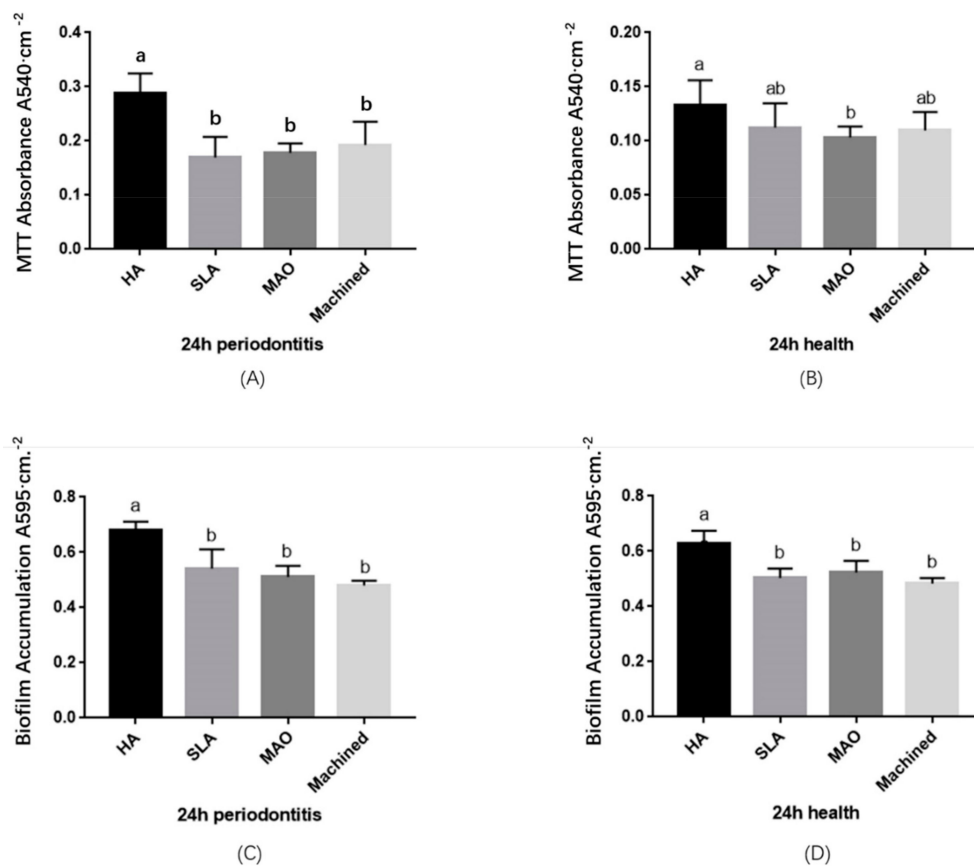


Figure 3. Biomass accumulation and metabolic activity of saliva-derived biofilms (periodontitis and health) on titanium discs. (A,B) The metabolic activity of saliva-derived biofilms ($n = 6$); and (C,D) the biomass accumulation of saliva-derived biofilms on titanium discs ($n = 6$). Significant differences between bars are marked with the letters a and b ($p < 0.05$).

3.4. Live/Dead Staining

The results of the live/dead bacteria staining are presented in Figure 4. More dead cells were detected on the MAO titanium discs in both the periodontitis group (Figure 4C) and the healthy group (Figure 4G). Moreover, the MAO titanium discs in both groups showed less biofilm thickness compared to the HA group ($p < 0.05$) (Figure 4K,L). When quantifying the fluorescence, the periodontitis group showed that the MAO group had a higher ratio compared to the other three groups (Figure 4I), however, no other significant differences were observed. Meanwhile, in the healthy group, the MAO titanium discs had a higher live/dead ratio compared to the HA titanium and machined titanium ($p < 0.05$) (Figure 4J). The data indicated that MAO titanium had a higher rate of dead cells in the biofilm.

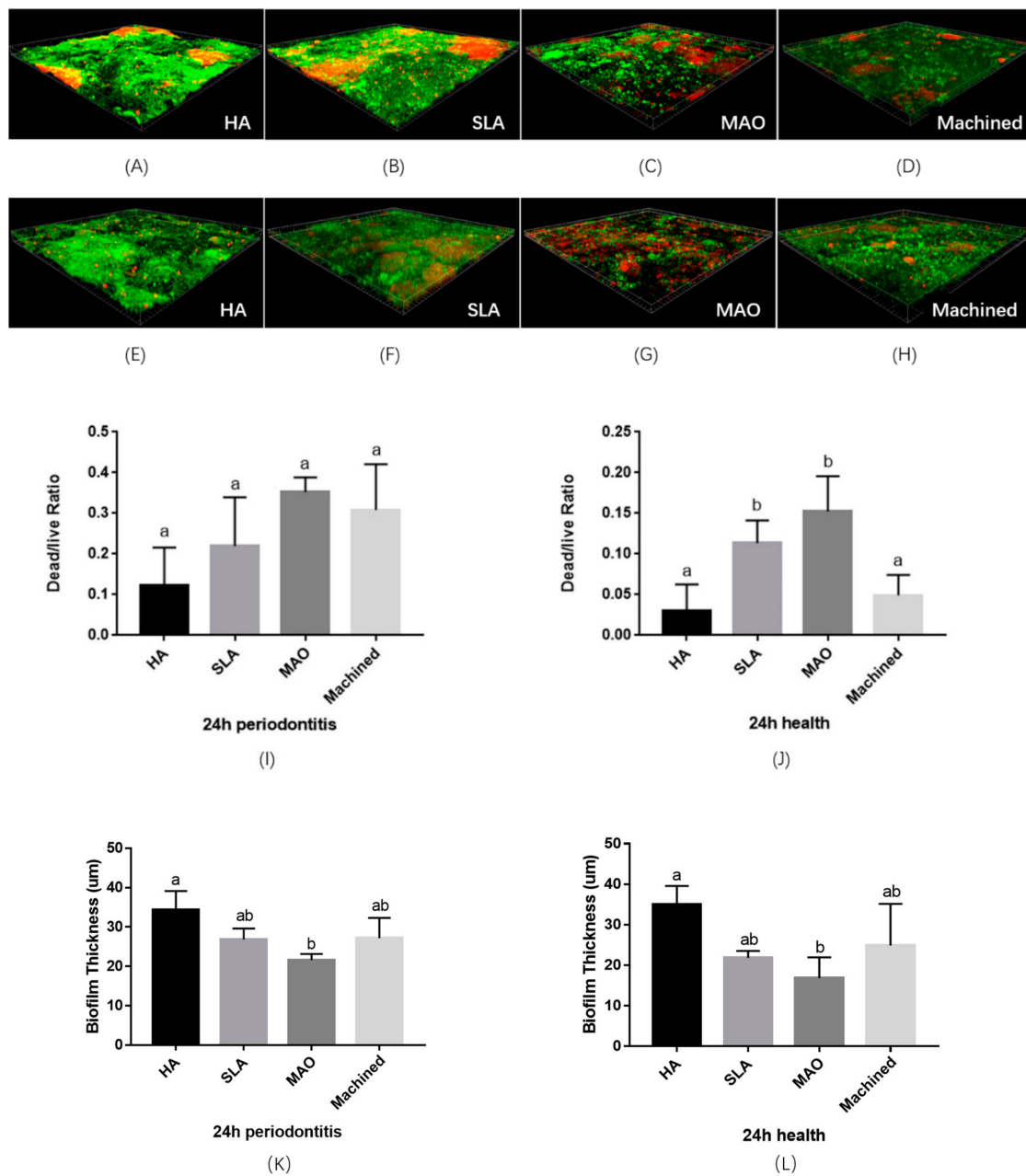


Figure 4. Confocal laser scanning microscope (CLSM) of saliva-derived biofilms. Live/dead staining of biofilms on titanium discs in the four groups. Live cells are stained green, whereas dead cells are stained red. (A,B,C,D) Periodontitis HA, SLA, MAO, and machined; (E,F,G,H) healthy HA, SLA, MAO, and machined; (I) live/dead ratio of periodontitis; (J) live/dead ratio of health; (K) biofilm thickness of periodontitis; and (L) biofilm thickness of healthy sample. Significant differences between bars are marked with different letters (a, b) ($p < 0.05$).

3.5. The Microbial Community of Saliva-Derived Biofilms

The 16S rDNA sequencing data of the periodontitis group is presented in Figure 5A–D. The Shannon index revealed that the machined group had a lower diversity of species ($p < 0.05$) (Figure 5A). In addition, the principal co-ordinates analysis (PCoA) showed that the biofilms of the four groups were distinctly separate from one another (Figure 5B). Moreover, after removing *Streptococcus*, the microbial composition of the four groups was different. A higher abundance of *Lactobacillus* was detected in the HA, SLA, and MAO group compared to the CP group ($p < 0.05$) (Figure 5C,D).

The data of the healthy group is presented in Figure 5E–H. The MAO group showed higher diversity compared to the other three groups in the Shannon index (Figure 5E), and the PCoA indicated separation from group to group, such as the periodontitis group (Figure 5F). Regarding microbial composition, the group showed a significantly higher rate of *Lactobacillus* compared to the HA, SLA, and the machined group ($p < 0.05$) after removing *Streptococcus* (Figure 5G,H).

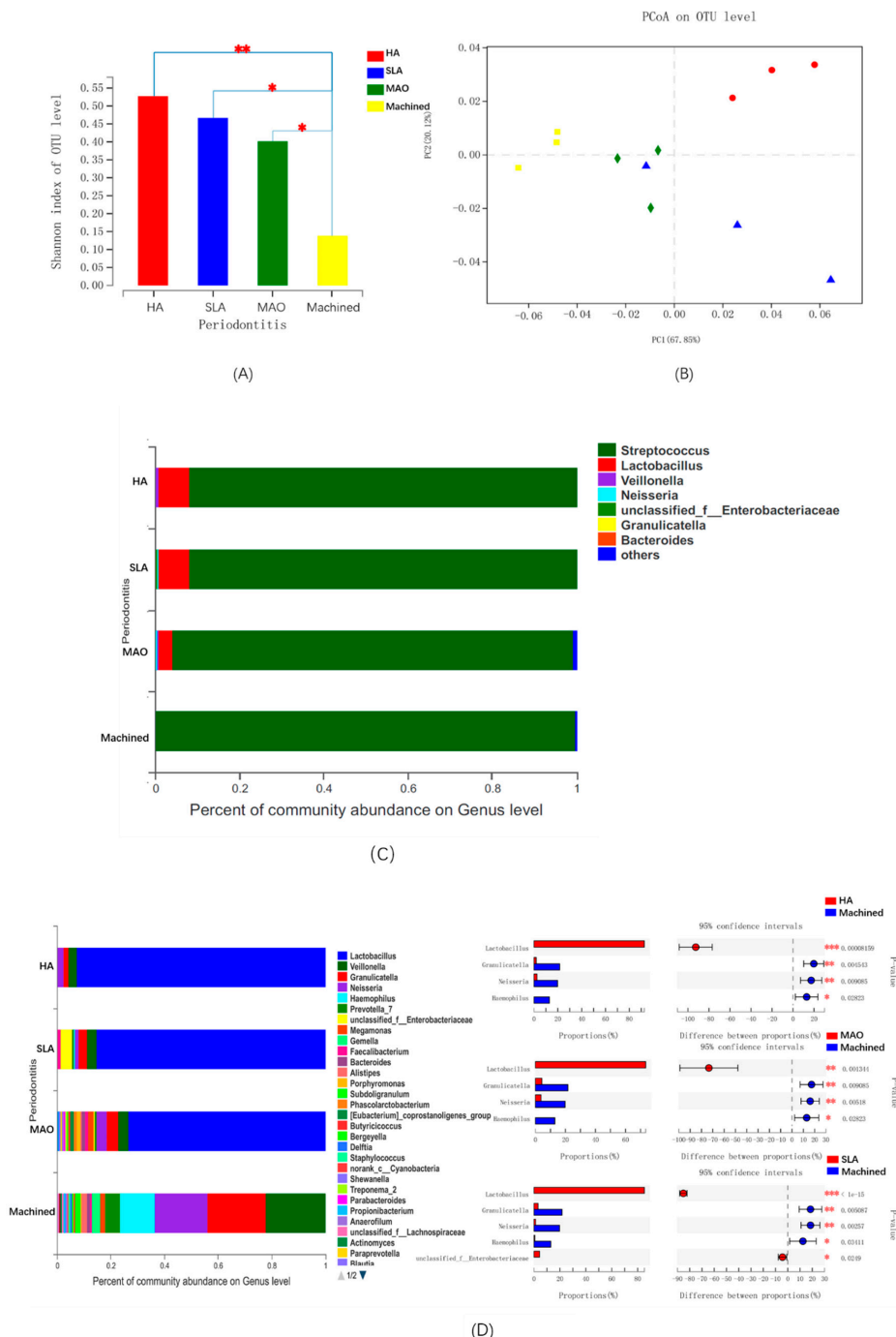


Figure 5. Cont.

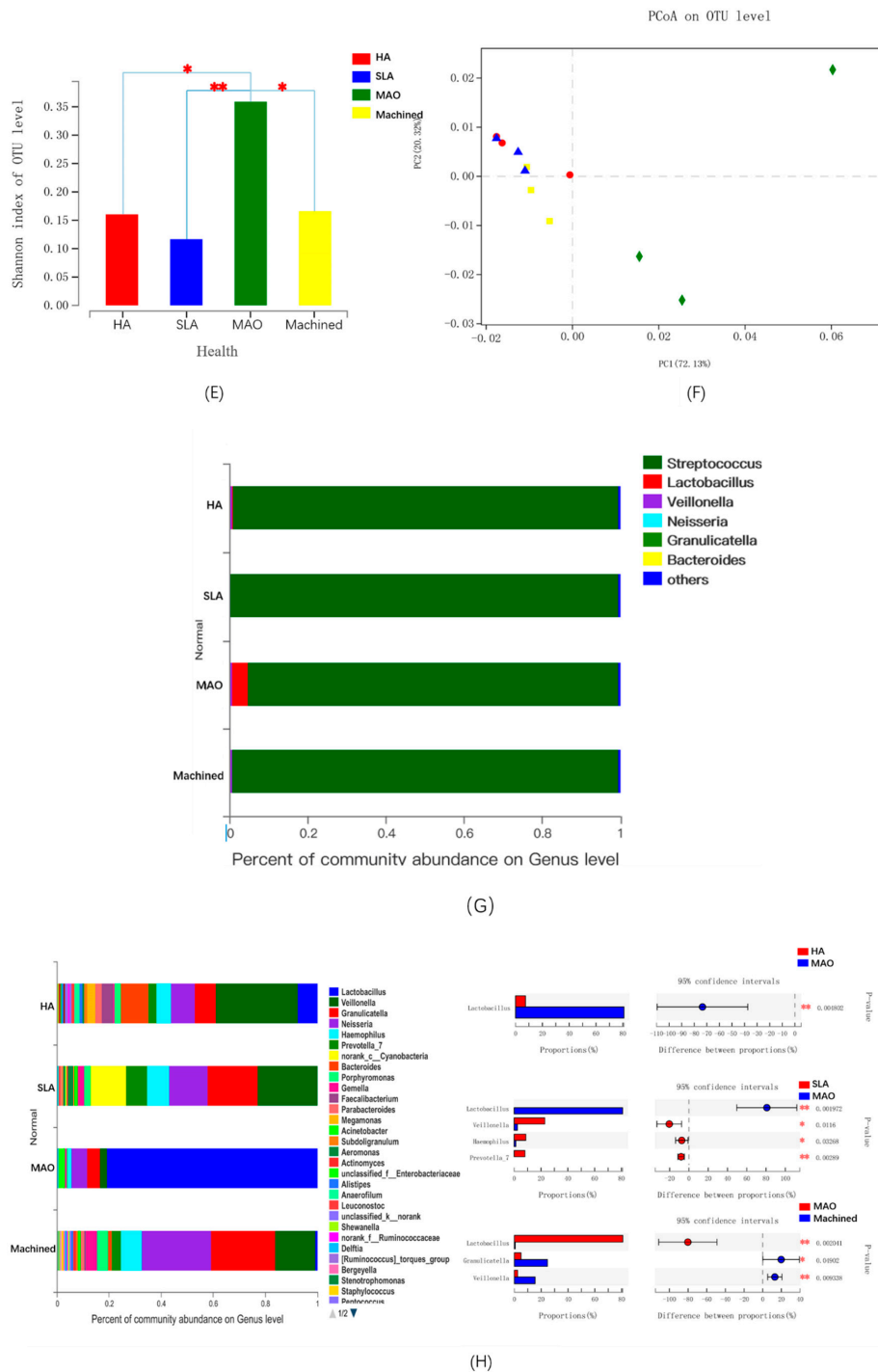


Figure 5. The microbial community of saliva-derived biofilms. **(A)** The alpha diversity of groups in the periodontitis group was measured using the Shannon index; **(B)** a principal co-ordinates analysis (PCoA) score plot of the HA (red), SLA (blue), MAO (green), and machined group (yellow) in the periodontitis group; **(C)** shows the percent of community abundance at the genus level in the periodontitis group; **(D)** Shows the percent of community abundance at the genus level after removing *Streptococcus*, and the comparison of two samples in the periodontitis group; **(E)** the alpha diversity of groups in the healthy group was measured using the Shannon index; **(F)** a principal co-ordinates analysis (PCoA) score plot of the HA (red), SLA (blue), MAO (green), and machined group (yellow) in the healthy group; **(G)** shows the percent of community abundance at the genus level after removing the *Streptococcus* from the healthy group; and **(H)** shows the percent of community abundance at the genus level and the comparison of two samples in the healthy group.

4. Discussion

In previous studies, controlled multi-species biofilm models have been used to evaluate the anti-peri-implantitis effect of modified dental implants in vitro [36–39]. However, the oral environment is a complex community and is composed of not only pathogenic bacteria but also beneficial bacteria, such as *Lactobacillus*. It has previously been reported that *Lactobacillus* protects the oral cavity from pathogenic periodontal microbes by forming a biofilm around dental tissue [40]. In several publications indicated, via numerous clinical studies, that *Lactobacillus* is a type of probiotic that prevents and treats peri-implant disease [11–13,41,42]. By preventing the growth of *Porphyromonas gingivalis* (*P. g*) and *Prevotella intermedia* (*P. i*) and by reducing the levels of cytokines related to inflammatory reactions, the periodontal parameters could be improved [13,43]. Peri-implantitis and periodontitis are both polymicrobial inflammatory diseases that may lead to destruction of the tissue supporting the tooth/implant. Without therapy, this may lead to loss of the tooth/implant [5,44]. In patients without a history of periodontitis, the implant had less bone loss and less inflammation in the long term [45]. In addition, periodontal pathogens are thought to be involved in the development of peri-implant inflammation [46]. Thus, these models have their limitations in testing the effect of novel dental implants on the microbial ecosystem of biofilms, especially with periodontitis from a patient's view. Thus, in this study, healthy and periodontitis saliva-derived biofilms cultured with an SHI medium that had been confirmed to be able to support a diversified oral microbial community of periodontitis and healthy individuals in vitro were selected [25,27]. Previous studies showed that the microbiota in saliva with periodontitis was different from that of the healthy group [47]. We obtained similar results and found that biofilms derived from saliva with periodontitis versus that of healthy people showed differences. There were more *Bacillus* in the periodontitis group and more *Coccus* in the healthy group (Figure 2), which may be due to the many periodontitis pathogenic *Bacillus* bacteria, such as *Fusobacterium nucleatum* (*F. n*), *Actinobacillus actinomycetemcomitans* (*A. a*).

Anodic oxidation is a method to establish an oxide film on a metal surface through discharge oxidation, which is a very mature means of surface modification of metal materials [48]. The generated metal oxide coating can change the surface color, corrosion resistance, hardness, and other properties of titanium-based materials. The layer of oxide generated a large amount of titanium hydroxyl on the surface of the titanium, and promoted the deposition of HA and the adhesion of osteoblasts [49]. The MAO technology is a modification method for in situ generation of bioactive coatings on the surface of non-ferrous metals, which is an upgrade from anodic oxidation technology. By adjusting the electrolyte and corresponding voltage or current parameters, and by taking advantage of the instantaneous high temperature effect that is generated by arc discharge, an oxide film with a thickness of tens of microns, a dense inner layer and a porous outer layer is formed on the surface of titanium [50]. This inner layer of dense outer porous oxide film can promote cell adhesion on the surface of the implant and enhance general adhesion. This treatment technology has been widely used in biomedical titanium improvement [48,50,51]. Our novel modified micro-arc oxidation, which was optimized according to surface color, microstructure, and biological activity [23,52], had a uniform surface (Figure 1). In addition, in our previous study, it proved to have better osteogenic characteristics [23,24]. Moreover, MAO titanium has no risk of surface shedding, such as that of HA titanium, and has no particle residual, such as that of SLA titanium. However, further microbiological evaluation is still lacking.

To evaluate the microbiological properties of a novel material, the number of bacteria, their metabolism, and their composition should be considered. In a previous study, the higher number of bacteria, stronger metabolism, and lower number of beneficial bacteria such as *Lactobacillus* indicated a greater possibility that the implant might result in peri-implantitis [14,25]. The diversity meant the self-regulation ability of the flora. Patrick et al. found that the modified SLA surface had a higher trend for six-species biofilm colonization compared to a machined surface [53]. To identify the microbiome on SLA titanium and machined titanium surfaces, Fabiana et al. exposed these two types of titanium to the oral environment of healthy people for 24 h, then used 16S rDNA sequencing for microbial community

analysis. In their results, no differences were found with regard to the operational taxonomic units (OTUs) and microbial diversity [54], which was similar to our findings. In Matos's three-species biofilm study, the count of *F. n* was lower for MAO treatment at the early biofilm phase, and the biofilm extracellular matrix was similar among the MAO, SLA, and machined titanium. Cell proliferation was not significantly affected by the experiment, except for that of MAO at six days, which resulted in increased cell proliferation [37]. In our findings of the healthy group, the metabolic activity of bacteria in the MAO group was lower compared to the HA group, SLA group, and machined group. Furthermore, the number of bacteria in the MAO group was smaller compared to that in the HA group (Figure 3B,D). The MAO group had the highest live/dead ratio of the four groups (Figure 4). Surprisingly, our findings showed that MAO titanium did not inhibit the growth of *Lactobacillus*, therefore, the relative abundance of *Lactobacillus* in the MAO group increased significantly compared to the other three groups, and the diversity index of the MAO group was also the highest of the other three groups (Figure 5D,F). Therefore, MAO titanium implants would be a potential option in healthy people. In the group of periodontitis, the relative abundance of *Lactobacillus* and the diversity index in the HA, SLA, and MAO groups was higher compared to that in the machined group (Figure 5A,C), which meant higher stability and controllability in the three types of titanium. Although, of the three groups, the HA group showed a higher number of bacteria and metabolic activity (Figure 3A,C), all in all there was no significant difference between the three titanium plates. Therefore, HA, SLA, and MAO titanium implants would be a good choice for patients with periodontitis.

5. Conclusions

In this study, we investigated, for the first time, the anti-biofilm and microecosystem-regulating effects of a novel micro-arc oxidation implant material. The novel MAO titanium not only inhibited the biomass accumulation and metabolic activity of saliva-derived biofilm, but also regulated the microbial ecosystem to a healthier condition. Therefore, the novel MAO dental implant is promising for the prevention of peri-implantitis through the inhibition of biofilms in an 'ecological way', especially allowing healthy people to combat peri-implantitis. However, due to the limitations of the in vitro studies, additional in vivo studies will be needed to reach definitive conclusions regarding this outcome.

Author Contributions: Conceptualization, L.C. and X.H.; methodology, X.H. and Y.H.; software, W.Z. and P.X.; validation, X.Z., B.Y., X.P. and B.R.; formal analysis, B.L.; writing—original draft preparation, X.H.; writing—review and editing, X.H.; supervision, L.C. and M.L.; project administration, L.C. and M.L.

Funding: This study was supported by the National Key Research and Development Program of China 2016YFC1102700 (X.Z.); the National Natural Science Foundation of China grant 81870759 (L.C.), and 81430011 (X.Z.); the Youth Grant of the Science and Technology Department of Sichuan Province, China 2017JQ0028 (L.C.); and the Innovative Research Team Program of Sichuan Province (L.C.).

Conflicts of Interest: The authors declare no conflicts of interest.

References

1. Robertson, K.; Shahbazian, T.; MacLeod, S. Treatment of peri-implantitis and the failing implant. *Dent. Clin. N. Am.* **2015**, *59*, 329–343. [[CrossRef](#)] [[PubMed](#)]
2. Mir-Mari, J.; Mir-Orfila, P.; Figueiredo, R.; Valmaseda-Castellon, E.; Gay-Escoda, C. Prevalence of peri-implant diseases. A cross-sectional study based on a private practice environment. *J. Clin. Periodontol.* **2012**, *39*, 490–494. [[CrossRef](#)] [[PubMed](#)]
3. Mameno, T.; Wada, M.; Onodera, Y.; Fujita, D.; Sato, H.; Ikebe, K. Longitudinal study on risk indicators for peri-implantitis using survival-time analysis. *J. Prosthodont. Res.* **2018**, *63*, 216–220. [[CrossRef](#)] [[PubMed](#)]
4. Schwendicke, F.; Tu, Y.K.; Stolpe, M. Preventing and Treating Peri-Implantitis: A Cost-Effectiveness Analysis. *J. Periodontol.* **2015**, *86*, 1020–1029. [[CrossRef](#)]
5. Lasserre, J.F.; Brex, M.C.; Toma, S. Oral Microbes, Biofilms and Their Role in Periodontal and Peri-Implant Diseases. *Materials* **2018**, *11*, 1802. [[CrossRef](#)]

6. Renvert, S.; Quirynen, M. Risk indicators for peri-implantitis. A narrative review. *Clin. Oral Implant. Res.* **2015**, *26* (Suppl. 11), 15–44. [[CrossRef](#)]
7. Lafaurie, G.I.; Sabogal, M.A.; Castillo, D.M.; Rincon, M.V.; Gomez, L.A.; Lesmes, Y.A.; Chambrone, L. Microbiome and Microbial Biofilm Profiles of Peri-Implantitis: A Systematic Review. *J. Periodontol.* **2017**, *88*, 1066–1089. [[CrossRef](#)]
8. Apatzidou, D.; Lappin, D.F.; Hamilton, G.; Papadopoulos, C.A.; Konstantinidis, A.; Riggio, M.P. Microbiome of peri-implantitis affected and healthy dental sites in patients with a history of chronic periodontitis. *Arch. Oral Biol.* **2017**, *83*, 145–152. [[CrossRef](#)]
9. Belkacemi, S.; Mazel, A.; Tardivo, D.; Tavitian, P.; Stephan, G.; Bianca, G.; Terrer, E.; Drancourt, M.; Aboudharam, G. Peri-implantitis-associated methanogens: A preliminary report. *Sci. Rep.* **2018**, *8*, 9447. [[CrossRef](#)]
10. Stokman, M.A.; van Winkelhoff, A.J.; Vissink, A.; Spijkervet, F.K.; Raghoobar, G.M. Bacterial colonization of the peri-implant sulcus in dentate patients: A prospective observational study. *Clin. Oral Investig.* **2017**, *21*, 717–724. [[CrossRef](#)]
11. Flichy-Fernandez, A.J.; Ata-Ali, J.; Alegre-Domingo, T.; Candel-Marti, E.; Ata-Ali, F.; Palacio, J.R.; Penarrocha-Diago, M. The effect of orally administered probiotic *Lactobacillus reuteri*-containing tablets in peri-implant mucositis: A double-blind randomized controlled trial. *J. Periodontol. Res.* **2015**, *50*, 775–785. [[CrossRef](#)] [[PubMed](#)]
12. Sajedinejad, N.; Paknejad, M.; Houshmand, B.; Sharafi, H.; Jelodar, R.; Shahbani Zahiri, H.; Noghabi, K.A. *Lactobacillus salivarius* NK02: A Potent Probiotic for Clinical Application in Mouthwash. *Probiotics Antimicrob. Proteins* **2018**, *10*, 485–495. [[CrossRef](#)] [[PubMed](#)]
13. Tada, H.; Masaki, C.; Tsuka, S.; Mukaibo, T.; Kondo, Y.; Hosokawa, R. The effects of *Lactobacillus reuteri* probiotics combined with azithromycin on peri-implantitis: A randomized placebo-controlled study. *J. Prosthodont. Res.* **2018**, *62*, 89–96. [[CrossRef](#)] [[PubMed](#)]
14. Silva, T.S.O.; Freitas, A.R.; Pinheiro, M.L.L.; do Nascimento, C.; Watanabe, E.; Albuquerque, R.F. Oral Biofilm Formation on Different Materials for Dental Implants. *J. Vis. Exp.* **2018**, *11*, 1802. [[CrossRef](#)] [[PubMed](#)]
15. Roehling, S.; Astasov-Frauenhoffer, M.; Hauser-Gerspach, I.; Braissant, O.; Woelfler, H.; Waltimo, T.; Kniha, H.; Gahlert, M. In Vitro Biofilm Formation on Titanium and Zirconia Implant Surfaces. *J. Periodontol.* **2017**, *88*, 298–307. [[CrossRef](#)] [[PubMed](#)]
16. Al-Ahmad, A.W.-A.-A.M.; Faust, J.; Bachle, M.; Follo, M.; Wolkewitz, M.; Hannig, C.; Hellwig, E.; Carvalho, C.; Kohal, R. Biofilm formation and composition on different implant materials in vivo. *J. Biomed. Mater. Res. B Appl. Biomater.* **2010**, *95*, 101–109. [[CrossRef](#)]
17. Bermejo, P.; Sanchez, M.C.; Llama-Palacios, A.; Figuero, E.; Herrera, D.; Sanz, M. Biofilm formation on dental implants with different surface micro-topography: An in vitro study. *Clin. Oral Implant. Res.* **2019**, *30*, 725–734. [[CrossRef](#)]
18. Zhao, B.; van der Mei, H.C.; Subbiahdoss, G.; de Vries, J.; Rustema-Abbing, M.; Kuijter, R.; Busscher, H.J.; Ren, Y. Soft tissue integration versus early biofilm formation on different dental implant materials. *Dent. Mater.* **2014**, *30*, 716–727. [[CrossRef](#)]
19. Scarano, A.P.M.; Caputi, S.; Favero, G.A.; Piattelli, A. Bacterial adhesion on commercially pure titanium and zirconium oxide disks: An in vivo human study. *J. Periodontol.* **2004**, *75*, 292–296. [[CrossRef](#)]
20. Namgoong, H.; Kim, M.D.; Ku, Y.; Rhyu, I.C.; Lee, Y.M.; Seol, Y.J.; Gu, H.J.; Susin, C.; Wikesjo, U.M.; Koo, K.T. Bone reconstruction after surgical treatment of experimental peri-implantitis defects at a sandblasted/acid-etched hydroxyapatite-coated implant: An experimental study in the dog. *J. Clin. Periodontol.* **2015**, *42*, 960–966. [[CrossRef](#)]
21. Madi, M.; Zakaria, O.; Ichinose, S.; Kasugai, S. Effect of Induced Periimplantitis on Dental Implants With and Without Ultrathin Hydroxyapatite Coating. *Implant. Dent.* **2016**, *25*, 39–46. [[CrossRef](#)] [[PubMed](#)]
22. Conserva, E.; Generali, L.; Bandieri, A.; Cavani, F.; Borghi, F.; Consolo, U. Plaque accumulation on titanium disks with different surface treatments: An in vivo investigation. *Odontology* **2018**, *106*, 145–153. [[CrossRef](#)] [[PubMed](#)]
23. Xiao, M.; Biao, M.; Chen, Y.; Xie, M.; Yang, B. Regulating the osteogenic function of rhBMP 2 by different titanium surface properties. *J. Biomed. Mater. Res. A* **2016**, *104*, 1882–1893. [[CrossRef](#)] [[PubMed](#)]
24. Yue, C.; Yang, B. Bioactive Titanium Surfaces with the Effect of Inhibiting Biofilm Formation. *J. Bionic Eng.* **2014**, *11*, 589–599. [[CrossRef](#)]

25. Li, B.; Ge, Y.; Wu, Y.; Chen, J.; Xu, H.H.K.; Yang, M.; Li, M.; Ren, B.; Feng, M.; Weir, M.D.; et al. Anti-Bacteria and Microecosystem-Regulating Effects of Dental Implant Coated with Dimethylaminododecyl Methacrylate. *Molecules* **2017**, *22*, E2013. [[CrossRef](#)]
26. Cheng, L.; Zhang, K.; Melo, M.A.; Weir, M.D.; Zhou, X.; Xu, H.H. Anti-biofilm dentin primer with quaternary ammonium and silver nanoparticles. *J. Dent. Res.* **2012**, *91*, 598–604. [[CrossRef](#)]
27. Li, B.; Zhou, X.; Zhou, X.; Wu, P.; Li, M.; Feng, M.; Peng, X.; Ren, B.; Cheng, L. Effects of different substrates/growth media on microbial community of saliva-derived biofilm. *FEMS Microbiol. Lett.* **2017**, *364*. [[CrossRef](#)]
28. Zhou, C.; Weir, M.D.; Zhang, K.; Deng, D.; Cheng, L.; Xu, H.H. Synthesis of new antibacterial quaternary ammonium monomer for incorporation into CaP nanocomposite. *Dent. Mater.* **2013**, *29*, 859–870. [[CrossRef](#)]
29. Zhou, X.; Wang, S.; Peng, X.; Hu, Y.; Ren, B.; Li, M.; Hao, L.; Feng, M.; Cheng, L.; Zhou, X. Effects of water and microbial-based aging on the performance of three dental restorative materials. *J. Mech. Behav. Biomed. Mater.* **2018**, *80*, 42–50. [[CrossRef](#)]
30. Wang, S.; Zhang, K.; Zhou, X.; Xu, N.; Xu, H.H.; Weir, M.D.; Ge, Y.; Wang, S.; Li, M.; Li, Y.; et al. Antibacterial effect of dental adhesive containing dimethylaminododecyl methacrylate on the development of *Streptococcus mutans* biofilm. *Int. J. Mol. Sci.* **2014**, *15*, 12791–12806. [[CrossRef](#)]
31. Ge, Y.; Ren, B.; Zhou, X.; Xu, H.H.K.; Wang, S.; Li, M.; Weir, M.D.; Feng, M.; Cheng, L. Novel Dental Adhesive with Biofilm-Regulating and Remineralization Capabilities. *Materials* **2017**, *10*, 26. [[CrossRef](#)] [[PubMed](#)]
32. Wang, A.H.; Li, M.; Li, C.Q.; Kou, G.J.; Zuo, X.L.; Li, Y.Q. Human colorectal mucosal microbiota correlates with its host niche physiology revealed by endomicroscopy. *Sci. Rep.* **2016**, *6*, 21952. [[CrossRef](#)] [[PubMed](#)]
33. Caporaso, J.G. QIIME allows analysis of highthroughput community sequencing data. *Na. Methods* **2010**, *7*, 335–336. [[CrossRef](#)] [[PubMed](#)]
34. Cole, J.R.; Chai, B.; Farris, R.J.; Wang, Q.; Kulam, S.A.; McGarrell, D.M.; Garrity, G.M.; Tiedje, J.M. The Ribosomal Database Project (RDP-II): Sequences and tools for high-throughput rRNA analysis. *Nucleic Acids Res.* **2005**, *33*, 294–296. [[CrossRef](#)]
35. Dewhirst, F.E.; Chen, T.; Izard, J.; Paster, B.J.; Tanner, A.C.; Yu, W.H.; Lakshmanan, A.; Wade, W.G. The human oral microbiome. *J. Bacteriol.* **2010**, *192*, 5002–5017. [[CrossRef](#)]
36. Oliveira, W.F.; Silva, P.M.S.; Silva, R.C.S.; Silva, G.M.M.; Machado, G.; Coelho, L.; Correia, M.T.S. *Staphylococcus aureus* and *Staphylococcus epidermidis* infections on implants. *J. Hosp. Infect.* **2018**, *98*, 111–117. [[CrossRef](#)]
37. Matos, A.O.; Ricomini-Filho, A.P.; Beline, T.; Ogawa, E.S.; Costa-Oliveira, B.E.; de Almeida, A.B.; Nociti Junior, F.H.; Rangel, E.C.; da Cruz, N.C.; Sukotjo, C.; et al. Three-species biofilm model onto plasma-treated titanium implant surface. *Coll. Surf. B Biointerfaces* **2017**, *152*, 354–366. [[CrossRef](#)]
38. Montelongo-Jauregui, D.; Srinivasan, A.; Ramasubramanian, A.K.; Lopez-Ribot, J.L. An In Vitro Model for *Candida albicans*(-)*Streptococcus gordonii* Biofilms on Titanium Surfaces. *J. Fungi* **2018**, *4*, 66. [[CrossRef](#)]
39. Gokmenoglu, C.; Kara, N.B.; Belduz, M.; Kamburoglu, A.; Tosun, I.; Sadik, E.; Kara, C. Evaluation of *Candida albicans* biofilm formation on various parts of implant material surfaces. *Niger. J. Clin. Pract.* **2018**, *21*, 33–37. [[CrossRef](#)]
40. Caglar, E.; Karqul, B.; Tanboga, I. Bacteriotherapy and probiotics' role on oral health. *Oral Dis.* **2005**, *11*, 131–137. [[CrossRef](#)]
41. Pena, M.; Barallat, L.; Vilarrasa, J.; Vicario, M.; Violant, D.; Nart, J. Evaluation of the effect of probiotics in the treatment of peri-implant mucositis: A triple-blind randomized clinical trial. *Clin. Oral Investig.* **2019**, *23*, 1673–1683. [[CrossRef](#)] [[PubMed](#)]
42. Alqahtani, F.; Alqahtani, M.; Shafqat, S.S.; Akram, Z.; Al-Kheraif, A.A.; Javed, F. Efficacy of mechanical debridement with adjunctive probiotic therapy in the treatment of peri-implant mucositis in cigarette-smokers and never-smokers. *Clin. Implant. Dent. Relat. Res.* **2019**, *21*, 734–740. [[CrossRef](#)] [[PubMed](#)]
43. Köll-Klais, P.; Mandar, R.; Leibur, E.; Marcotte, H.; Hammarstrom, L.; Mikelsaar, M. Oral lactobacilli in chronic periodontitis and periodontal health: Species composition and antimicrobial activity. *Oral Microbiol. Immunol.* **2005**, *20*, 354–361. [[CrossRef](#)] [[PubMed](#)]
44. Sanz-Martin, I.; Doolittle-Hall, J.; Teles, R.P.; Patel, M.; Belibasakis, G.N.; Hammerle, C.H.F.; Jung, R.E.; Teles, F.R.F. Exploring the microbiome of healthy and diseased peri-implant sites using Illumina sequencing. *J. Clin. Periodontol.* **2017**, *44*, 1274–1284. [[CrossRef](#)]

45. Kroger, A.; Hulsmann, C.; Fickl, S.; Spinell, T.; Huttig, F.; Kaufmann, F.; Heimbach, A.; Hoffmann, P.; Enkling, N.; Renvert, S.; et al. The severity of human peri-implantitis lesions correlates with the level of submucosal microbial dysbiosis. *J. Clin. Periodontol.* **2018**, *45*, 1498–1509. [[CrossRef](#)]
46. Cortelli, S.C.; Cortelli, J.R.; Romeiro, R.L.; Costa, F.O.; Aquino, D.R.; Orzechowski, P.R.; Araujo, V.C.; Duarte, P.M. Frequency of periodontal pathogens in equivalent peri-implant and periodontal clinical statuses. *Arch. Oral Biol.* **2013**, *58*, 67–74. [[CrossRef](#)]
47. Belstrøm, D.; Fiehn, E.; Nielsen, C.H.; Kirkby, N.; Twetman, S.; Klepac-Ceraj, V.; Paster, B.J.; Holmstrup, P. Differences in bacterial saliva profile between periodontitis patients and a control cohort. *J. Clin. Periodontol.* **2014**, *41*, 104–112. [[CrossRef](#)]
48. Du, Q.; Wei, D.; Wang, Y.; Cheng, S.; Liu, S.; Zhou, Y.; Jia, D. The effect of applied voltages on the structure, apatite-inducing ability and antibacterial ability of micro arc oxidation coating formed on titanium surface. *Bioact. Mater.* **2018**, *3*, 426–433. [[CrossRef](#)]
49. Xiao, M.; Chen, Y.M.; Biao, M.N.; Zhang, X.D.; Yang, B.C. Bio-functionalization of biomedical metals. *Mater. Sci. Eng. C Mater. Biol. Appl.* **2017**, *70*, 1057–1070. [[CrossRef](#)]
50. Xu, L.; Zhang, K.; Wu, C.; Lei, X.; Ding, J.; Shi, X.; Liu, C. Micro-Arc Oxidation Enhances the Blood Compatibility of Ultrafine-Grained Pure Titanium. *Materials* **2017**, *10*, 1446. [[CrossRef](#)]
51. Yuan, X.; Tan, F.; Xu, H.; Zhang, S.; Qu, F.; Liu, J. Effects of different electrolytes for micro-arc oxidation on the bond strength between titanium and porcelain. *J. Prosthodont. Res.* **2017**, *61*, 297–304. [[CrossRef](#)] [[PubMed](#)]
52. Yang, B. Preparation of bioactive titanium metal via anodic oxidation treatment. *Biomaterials* **2004**, *25*, 1003–1010. [[CrossRef](#)]
53. Schmidlin, P.R.; MÜLLer, P.; Attin, T.; Wieland, M.; Hofer, D.; Guggenheim, B. Polyspecies biofilm formation on implant surfaces with different surface characteristics. *J. Appl. Oral Sci.* **2013**, *21*, 48–55. [[CrossRef](#)] [[PubMed](#)]
54. De Melo, F.; do Nascimento, C.; Souza, D.O.; de Albuquerque, R.F. Identification of oral bacteria on titanium implant surfaces by 16S rDNA sequencing. *Clin. Oral Implant. Res.* **2017**, *28*, 697–703. [[CrossRef](#)] [[PubMed](#)]



© 2019 by the authors. Licensee MDPI, Basel, Switzerland. This article is an open access article distributed under the terms and conditions of the Creative Commons Attribution (CC BY) license (<http://creativecommons.org/licenses/by/4.0/>).